Available online at www.sciencedirect.com
ScienceDirect
Trans. Nonferrous Met. Soc. China 20(2010) 2100−2110
Transactions of Nonferrous Metals Society of China
www.tnmsc.cn

Precision bending of high-quality components for volume applications

T. WELO, F. WIDERØE

Department of Engineering Design and Materials, Norwegian University of Science and Technology (NTNU), Richard Birkelands veg 2B, N-7491 Trondheim, Norway

Received 23 October 2009; accepted 30 March 2010

Abstract: Recent new technology developments were presented in the field of industrial bending operations, including flexible stretch forming and 3D rotary stretch forming. Attempts were made to give an overview of different mechanisms that influence dimensional accuracy, including local cross-sectional deformations such as suck-in and volume conservation effects, along with global deformations such as springback. An analytical model was developed to determine the particular influence of different material, geometry and process parameters on dimensional variability of bent components. The results were discussed in terms of overall process capability (C_p) and associated process windows. The results show that different governing mechanisms prevail in various bending operations, meaning that attention has to be placed on controlling those process parameters that really are important to part quality in each specific case. Several strategies may be defined for reducing variability. One alternative may be to design more robust process and tool technology that reduce the effect of upstream parameters on dimensional variability of the formed part. The results show that optimal tool design and technology may in specific cases improve the dimensional accuracy of a formed part. Based on the findings discussed herein, it is concluded that advances in industrial bending operations require focus on improving the understanding of mechanical mechanisms, including models and parameter development, new technology developments, including process, tool, measurement and control capabilities, and process discipline at the shop floor, combined with a basic philosophy of controlling process parameters rather than part attributes.
Key words: bending technology; tools; dimensional accuracy; distortions; springback; formability

1 Introduction

As a result of intensified globalization and increased cost pressure, manufacturing companies are forced to develop new strategies. By developing more advanced and automated production technology, providing reduced cost while improving product quality, these challenges may be met. Hence, the future competitiveness of manufacturing companies is strongly connected to their capability in developing and industrializing new technology, followed by commercialization into a stream of products that provide superior value to customers.

Industrial forming is one area where the pursuit for new technology may create advantages in the market place by offering products with higher added value. Improved bending technology is one way of achieving this by introducing forming capabilities that improve dimensional accuracy and reduce manufacturing and assembly time and cost in e.g. the automotive industry. In addition to extreme cost focus in the automotive industry, there is also an increasing pressure for making more environmentally friendly cars while simultaneously meeting customer demands of new safety and luxury features. Utilizing traditional manufacturing technologies, the most straightforward approach—but not always the optimal one — is reducing the weight of selected individual components to compensate for these additional features.

Aluminum extrusions represent one of several material alternatives that may provide considerable weight savings at reasonable cost penalty as compared with traditional materials, such as steel, as well as more modern materials such as magnesium alloys and composites. By using optimized product design and new advanced manufacturing technology (within a lean manufacturing framework), it may be possible to deliver more value to the customer by reducing weight and cost of components and assemblies. A main disadvantage of aluminum compared with traditional steel is its much higher material price, hence for high volume applications, where the material cost represents a major portion of the

Corresponding author: T. WELO; E-mail: torgeir.welo@ntnu.no
DOI: 10.1016/S1003-6326(09)60425-8

product cost, customers still have to be willing to pay a cost premium for achieving weight saving by selecting an aluminum part instead of a steel one. For low volume applications, light weight materials may be more cost competitive due to less impact of material price and more from tooling costs, product development, design solutions, etc. The main challenge for suppliers of light weight material components and products is to shift competitiveness (benefit-to-cost ratio) of their products to higher volumes.

The objective of this work is to demonstrate that new forming technology development, with a strong basis in mechanisms and models, is a key enabler towards the use of more environmental-friendly products, such as those made from aluminum alloys. Attempts have been made to start with some typical products and basic quality requirements, and bring these into a framework of dimensional strategies and forming technologies for meeting such demands. Principles related to bending tool design and mechanisms are discussed in terms of best practice. A model for prediction of dimensional characteristics in a cross section is presented and discussed in relation to key influential parameters. The applicability of the model is demonstrated on a new, fundamentally different forming technology: rotary stretch bending, focusing on the impact of material's anisotropy on cross sectional distortions.

2 Product quality

2.1 Product complexity

Several extrusion-based aluminum alloy products, including bumper systems, seat frame structure, engine cradle, sub frames and space frame, are shown in Fig.1. The complexity of each product is closely linked to specific functional and quality requirements, the number of individual parts included in the assembly as well as the number of subsequent process steps used in the manufacturing route. For example, a bumper beam consists basically of one single component which is manufactured in a process route that includes extrusion, sawing, (solution heat treatment), bending, piercing, machining and heat treatment. A sub-frame is significantly more complex since this product may include about thirty individual components going through the same process as a bumper beam before being machined, assembled, welded, post machined and surface treated.

For a sub-frame assembly, like the engine cradle and the windshield frame shown in Fig.1, the key is to understand the upstream and in-process parameters that control the dimensional accuracy of each component that enters into the final product. Moreover, the assembly

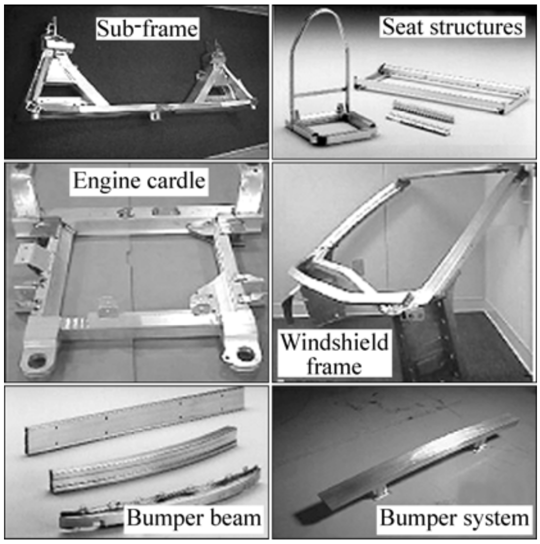

Fig.1 Structural extrusion-based aluminium alloy product examples

operations have to be done in an optimal sequence, allowing dimensional variations to be taken up along slip planes at common nodes where (MIG) welds are used for joining. It is essential to bring weld gaps down to a minimum (less than 0.25−0.4 mm) to ensure high-quality welds and consistent thermally-induced distortions. In addition, individual part and assembly fixtures have to provide a datum structure that is common with the datum structure of the final product that goes into the vehicle.

2.2 Dimensional accuracy

Dimensional tolerance capability of automotive structures is usually discussed in terms of two related parameters: 1) the process capability, C_p, and 2) the capability index, C_k. With reference to Fig.2, the process capability for a specific dimensional feature is defined as

$$C_p = \frac{L_U - L_L}{6D_S} \tag{1}$$

where L_U and L_L are the upper and lower specified tolerance limits for a given dimensional feature,

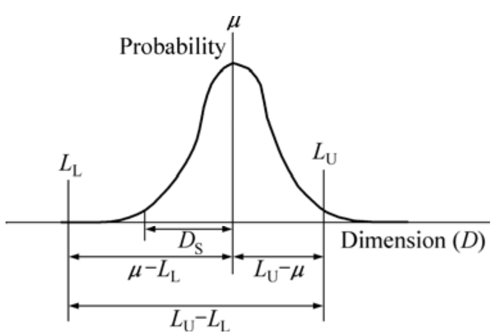

Fig.2 Parameters used to calculate process capability (C_p) and product capability index (C_k)

respectively, and D_S is the standard deviation derived from measurement data. Sufficient process control usually requires that C_p>1.33.

The dimensional metric defined above provides information on process capability only, and not targeting; in principle, from Eq.(1), process capability may still be high although no parts are made to print. Therefore, an additional requirement, which is known as the (product) capability index, is commonly used to define dimensional quality characteristics:

$$C_k = \left\{ \frac{|L_U - \mu|}{3D_S}, \frac{|\mu - L_L|}{3D_S} \right\}_{\min} \quad (2)$$

The capability index covers both process variation and targeting. It has usually to be greater than 1.33 for standard features and 1.67 for critical features (ones that are defined to be of key importance to the functionality and performance of product) according to automotive standards. It may be noticed that if targeting is perfect (nominal is consistent with math data) and the distribution is symmetric, the process capability and capability index provide the same value. In practice, however, C_k is always less than C_p, due to the difficulty in targeting the nominal of a dimensional feature equal to the characteristic value given.

3 Bending technologies

3.1 Industrial bending processes

Press bending, as shown in Fig.3(a), is a high speed forming operation that is well-suited for volume production. The process is typically used for relatively thick-walled sections, bars and open sections. However, tolerances and bend appearance are not very good.

Compression bending is done by clamping the work piece to a die, and using a wiper shoe to rotate the profile around the fixed bending die. Dimensional accuracy is low to moderate due to heavy shear forces and lack of stretching, as shown in Fig.3(b).

Stretch bending (Fig.3(c)) is efficient for forming of multiple bends in one single setup. The method applies to high volume production. Sometimes internal mandrels are used to minimize local distortions.

Rotary draw bending (Fig.3(d)) is well-suited for precision forming at tight radii. A constant bending moment along the bend generates low contact stresses between the part and the tool, thus minimizing distortions. A drawback associated with this process is the need for a sufficiently long profile, and a constant bending radius configuration.

Roll bending (Fig.3(e)) is typically used for prototyping and other low volume applications. It is well suited for large radius bends, but the precision of the bend is relatively low due to heavy contact stresses

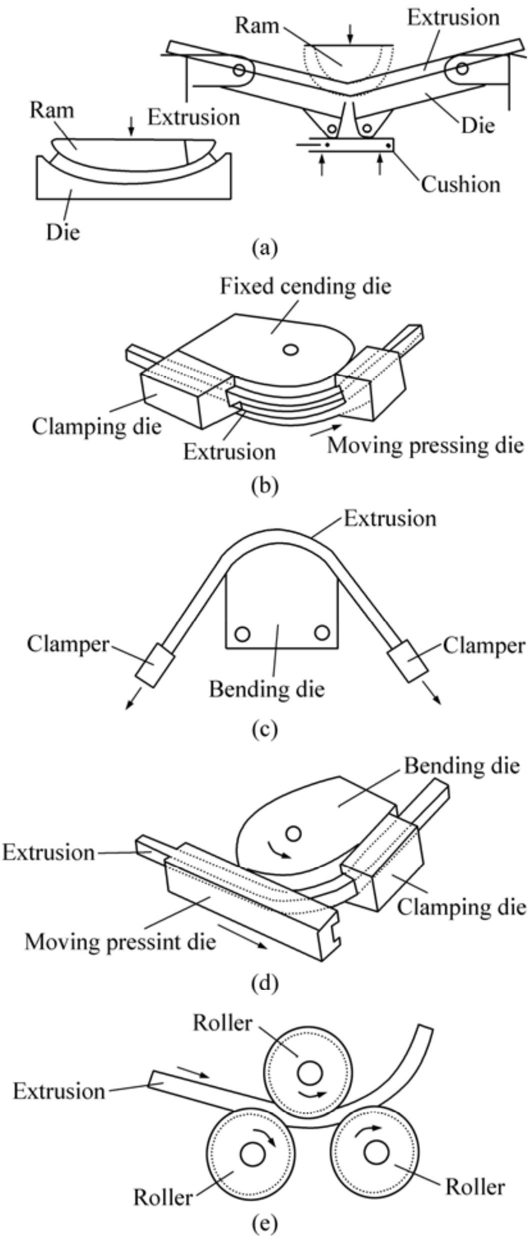

Fig.3 Some basic bending processes: (a) Press bending; (b) Compression bending; (c) Stretch forming; (d) Draw bending; (e) Roll bending

resulting from the short distance between the rolls. Springback compensation is also somewhat complicated.

There are pros and cons associated with each one of the bending processes presented above[1]. Some are attractive for dimensional accuracy, while others offer low part cost or tool cost. In industrial practice, therefore, hybrid processes, representing a compromise between investment, tooling cost, cycle time, tolerance capability, reliability and robustness, have evolved over the years.

3.2 Rotary stretch bending

Rotary stretch forming is an example of a hybrid process, which combines principles from draw bending and conventional stretch bending. The setup may include a stand-alone machine operated with integrated hydraulics, or a separate tool where an external (vertical) hydraulic press is used to generate tool movements. The latter alternative is more flexible for producing multiple products in the same manufacturing setup, while the former may provide less investment (and production cost) for dedicated products. A rotary stretch bending tool may be modular by using part specific inserts (mandrels and dies) and reusing the base tool between different part geometries. This requires, however, a disciplined approach for tool change-over procedures.

A rotary stretch forming tool concept consists of four different subsystems (Fig.4): 1) the upper tool (not shown in the figure), 2) the clamp/mandrel, 3) two lower counter rotating part-specific dies and 4) the base tool. In a setup with an external hydraulic press, the upper tool transfers the movement of the press to the lower tool. This action includes clamping the part to lock both ends relative to the lower die, using a mandrel type arrangement. Upon further press movement, the two semi dies are counter rotated about their individual pivot point. The clamped ends in combination with the rotation gradually form the inner face of the part into the configuration of the dies. A mechanical stop is normally used to control the final rotational angle of the two semi dies. The final step includes unloading by releasing the clamp and reversing the press movement; i.e., allowing the part spring back as a result of recovery in (elastic) stresses.

The main advantage of rotary stretch forming is

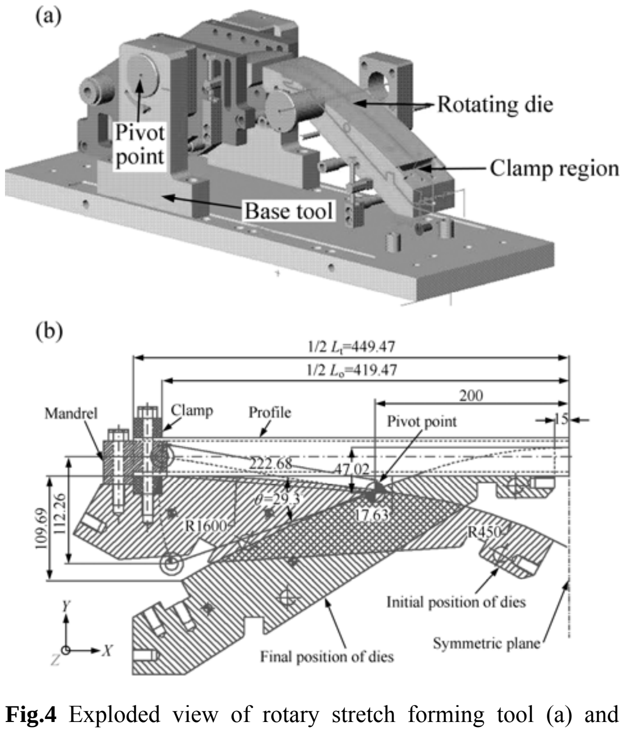

Fig.4 Exploded view of rotary stretch forming tool (a) and details of left semi die (b)

reduced springback (curvature) due to the simultaneous application of stretching and bending. Due to less nominal springback, the variations in springback as a result of process noise will also decrease, resulting in better dimensional accuracy of the product. Moreover, rotational movements of the semi dies reduce transverse shear forces as compared with those in traditional stretch forming, minimizing distortions such as crushing of the cross section due to heavy contact stresses.

The key to minimize springback is designing the tool in such a way that it, firstly, provides a suitable stretch level; too large stretch may cause formability problems (material or local distortions), whereas too low stretch tends to increase springback. Traditionally, tool makers aim at achieving a final strain of 0.5%−1.0% at the fibers located at the inner face of the profile's bend. Secondly, the inner flange of the profile must undergo a proportional straining process. It is particularly important to prevent (local) unloading towards the final stage of forming. On the contrary, just minor unloading results in a major shift in stress distribution across the section, which in turn increases the internal bending moment as well as the magnitude of springback and thus variations in springback. Tool designers use different approaches to prevent the undesirable effects of non-proportional stretching, for example, introducing an additional step that includes over-stretching of the part just before unloading. Another method is integrating cam (shaft) type actions in the base tool to allow controlled movement of the pivot points during the bending sequence. However, this makes the tool more complex and vulnerable to wear. The most straightforward and inexpensive method is to apply fixed pivot point positions, whose optimal location is determined based on the desired straining history of the part. One example is shown in Fig.5, which compares two alternative pivot point positions for a tool used for forming of bumper beams for a US automaker. The upper curve in Fig.5(a) shows that the inner flange of the beam is stretched nicely up to, say, half the maximum die rotation, from which the length of the inner flange is gradually shortened. Looking at the initial and final length, without the intermediate history in mind, it looks like the wanted stretching level of 0.5%−1.5% is achieved. However, consulting the lower curve in Fig.5(a), which shows (longitudinal) bending stress vs bending strain (elongation) throughout the bending sequence, a major shift in stress occurs as a result of unloading. At the point where the shortening of the flange starts, the equivalent stress becomes less than that of the instantaneous yield stress of the material, resulting in elastic unloading with a considerable change in the stress state. When the bending sequence is completed, the inner flange turns into compression. This results in a large bending moment

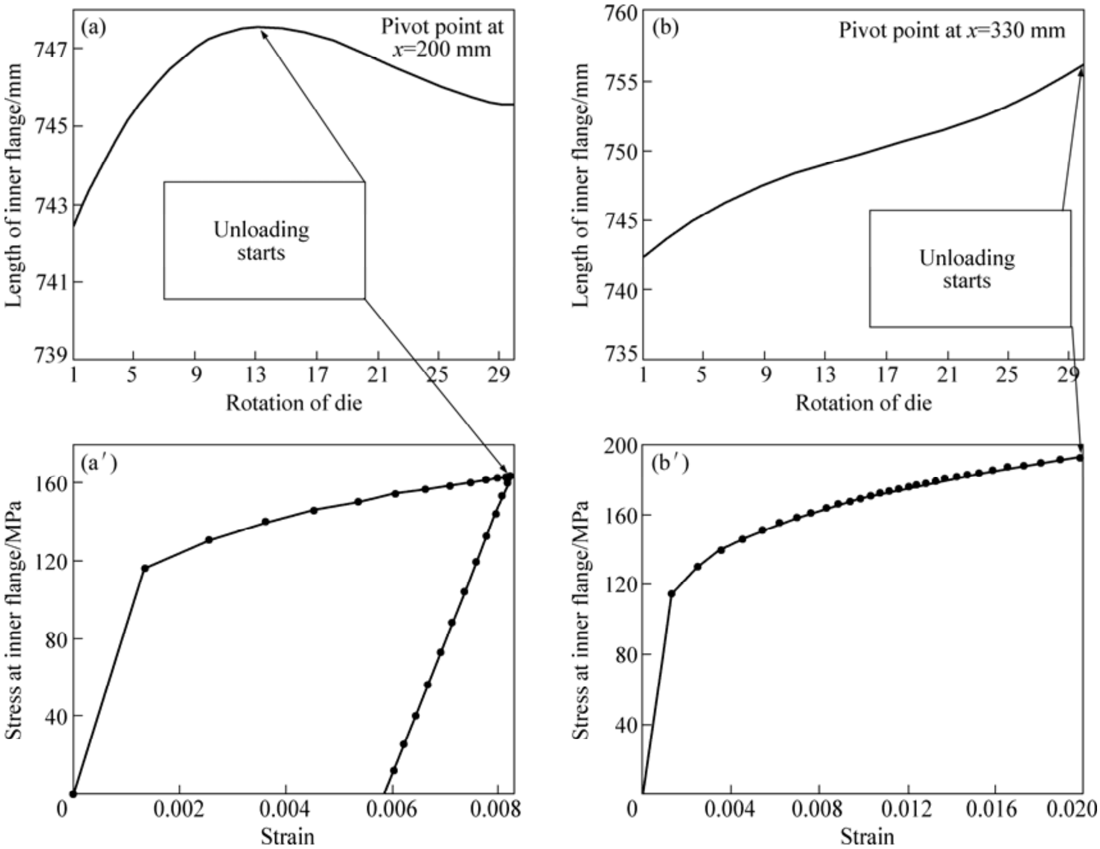

Fig.5 Tool design that results in unloading (a, a′) and more optimal tool design without unloading (b, b′)

and considerable springback—the favorable effect of stretching is more or less wiped out.

In Fig.5(b), the pivot points are moved 260 mm further apart. The results show that no flange shortening occurs; neither does unloading take place and the stress at the inner flange remains in tension at the instance of unloading, resulting in less springback. Results from this case show that springback and sweep tolerances are 4−5 times better for the latter die configuration. This benefit is achieved just by identifying a more optimal position of the pivot points with regard to achieving proportional straining throughout the process.

Reducing complexity while minimizing cycle time by combining simple motions into multiple functions is an important principle for a successful rotary stretch forming tool design. Modern stretch forming tools may operate at cycle times less than 8−10 s per part; in some cases, cycle time may be significantly lower when multiple parts are formed at the same time. Another key principle is avoiding internal mandrels other than the ones needed for clamping at the very end of the product. Long rigid finger mandrels and flexible mandrels used to provide internal support to the cross section upon bending have a tendency to create additional maintenance issues, variations in friction/lubrication (and hence springback) as well as figure at the top of the downtime-cause list. In addition, mandrels increase cycle time and hence part costs. Therefore, attempts should be made to avoid the (theoretical) need for internal mandrels by focusing on tool and part geometry design considerations in early design for manufacturability (DFM) feasibility events. One should also be aware of the fact that the application of stretching in rotary stretch bending does reduce springback in bending (curvatures) but at the expense of springback in the longitudinal direction of the part. Therefore, dimensional accuracy of part length (end-to-end location) will be affected by, say, variations in mechanical properties of the incoming profiles. If tight part length tolerance requirements prevail, the best strategy is to define small process windows for incoming material or, alternatively, to cut the part into length after the bending operation.

4 Mechanisms and interpretations

4.1 Challenges in industrial bending

More fundamental knowledge has to be established in order to fully understand mechanisms associated with different problems in bending, including (Fig.6): 1) material's formability, 2) local geometrical defects such as wrinkling and sagging of individual cross-sectional members, 3) global dimensional accuracy, including

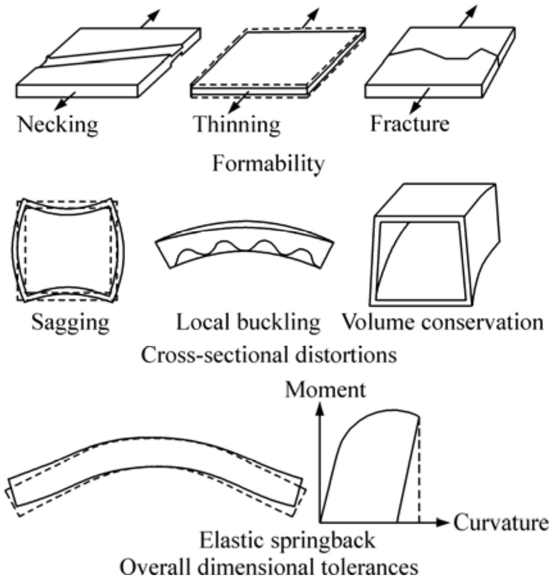

Fig.6 Challenges related to manufacturing of bent components

springback.

Formability of profiles in bending is generally related to mechanical properties of the material, geometry of the cross section as well as bending method. For example, necking or ductile fracture may from time to time occur for bending at tight radii, particularly when using stretch forming or press forming. However, formability (e.g. critical strain level) is different from that in uniaxial tension; specific material parameters, such as anisotropy, along with strain distribution and history may influence failure mode (e.g. diffused or localized necking). The important material's formability parameters are strain hardening, yield stress (level), anisotropy and strain rate sensitivity.

Local geometrical defects are essential to aesthetics, functional and performance characteristics as well as dimensional accuracy of the product, particularly in regions where surfaces have to meet up with surfaces of other components, e.g. for welding purposes. In stretch forming, local buckling of the inner flange may be eliminated, but at the expense of necking and dimensional problems of the external flange.

Elastic springback determines the global dimensional accuracy of bent components. Dealing with springback is a great challenge in manufacturing. The key is to establish tight control throughout the process route, providing consistent mechanical properties and forming conditions. The fact that aluminium alloy is an engineered material makes its yield characteristics extremely sensitive to processing conditions. Since the amount of springback in one way or another, depending on bending process, is related to the yield characteristics, the dimensional accuracy is directly affected by variability in the processing route. In summary, the manufacturer's concerns related to part quality of formed products are primarily repeatability, i.e. controlling and minimizing the effect of noise parameters and secondarily formability i.e. choosing the optimal design parameters that maximize formability of the component.

4.2 Local distortions

Considering the external flange of a profile bent at a constant die radius, the longitudinal stress level at its mid-plane (σ_x) may be calculated by assuming that initially plane sections remain plane during bending (Navier-Bernoulli), in combination with a suitable stress−strain model. Since the flange is deformed into a (constant) curvature, an inward-acting stress component of magnitude $\sigma_z=\sigma_x t_f/R$ occurs. Here t_f is the thickness of the flange and R is the radius of curvature. The system resembles the one of an infinitely long sheet, with a load applied at its two short edges, being inelastically constrained along its other two edges and loaded with a distributed load ($q=\sigma_z$). Under these conditions, the sheet will deform into a double curvature configuration in terms of global curvature (κ_y) and local curvature (κ_x) in the perpendicular direction. The latter is known as sagging or suck-in, and is shown for a single chamber cross section in Fig.7. From the interpretation above, the magnitude of sagging is related to the instantaneous inelastic bending stiffness of the flange, as represented by thickness, width, stress level, material characteristics, etc. Moreover, since the flange is rotationally constrained to the webs at both ends, the local bending stiffness of the webs influences the magnitude of sagging.

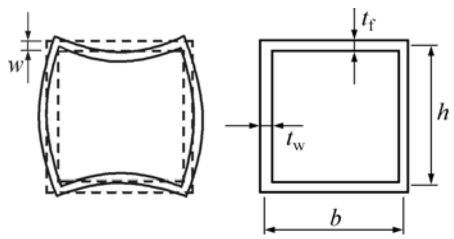

Fig.7 Local deformations (sagging) of cross section during bending

The interpretation above is also valid for bending processes other than pure bending. In rotary stretch bending, for example, the instantaneous local bending stiffness of the webs and the flange is less than that in pure bending due to higher principal strain levels. Therefore, increased sagging of the outer flange of the bend is one drawback associated with stretch bending. This may result in increased impact from noise factors that are quite different from those influencing springback. Moreover, the inner flange will deform quite differently from the outer flange; in case that stretching prevails across the entire depth of the profile, the 'distributed load

(q)' will tend to bend the inner flange in the direction of the neutral layer which is located at the inside of the inner face of the bend. However, the die surface constrains the flange from bending in this direction, meaning that the inner flange will remain flat. In the continuation, a more detailed discussion on effects of material's anisotropy on sagging will be given as a part of an application example.

A practical design method, based on analytical modelling of the sagging mechanism of the cross section, has been established[2]. The method represents an engineering solution of a relatively complex problem, and is illustrated for a hollow section in Fig.8. The method is applicable for both stretch forming and more conventional bending. The first step in determining the magnitude of sagging is to calculate the relative stretch level l/l_0, where l is the length of the profile taken at the mid-depth of the cross section in the fully stretched configuration, and l_0 is the initial length of the profile. The next step is to calculate the profile's depth-to-bend radius ratio ($h/2R$), and determine the parameter 'a' from the design chart in Fig.8(a). It should be noticed that a=1.0 corresponds to pure bending (l=l_0), whereas the special case with the neutral axis located just inside the inner flange corresponds to a=0.5. Entering the lower chart with the web-to-flange thickness ratio (t_w/t_f), the maximum sagging (w_{0s}) can be found by the procedure illustrated in Fig.8(b). This includes identification of the intersection points with the two families of curves based on the parameters, ab/h and $b^4/(t_f^2R^2)$, respectively. In addition to assessing nominal sagging depth, the procedure can be used to determine the expected variation in sagging due to change in, say, selected geometric dimensions.

5 Models and applications

5.1 General notes

In the continuation, an application example will be provided to demonstrate the applicability of the models, mechanisms and interpretations discussed above. The overall motivation is to show that the integration of knowledge and technology is a powerful combination for improving product quality (dimensional capability). This is believed to be a sustainable strategy for strengthening the position of manufacturing companies in today's competitive market place.

A mechanism that has to be considered in profile

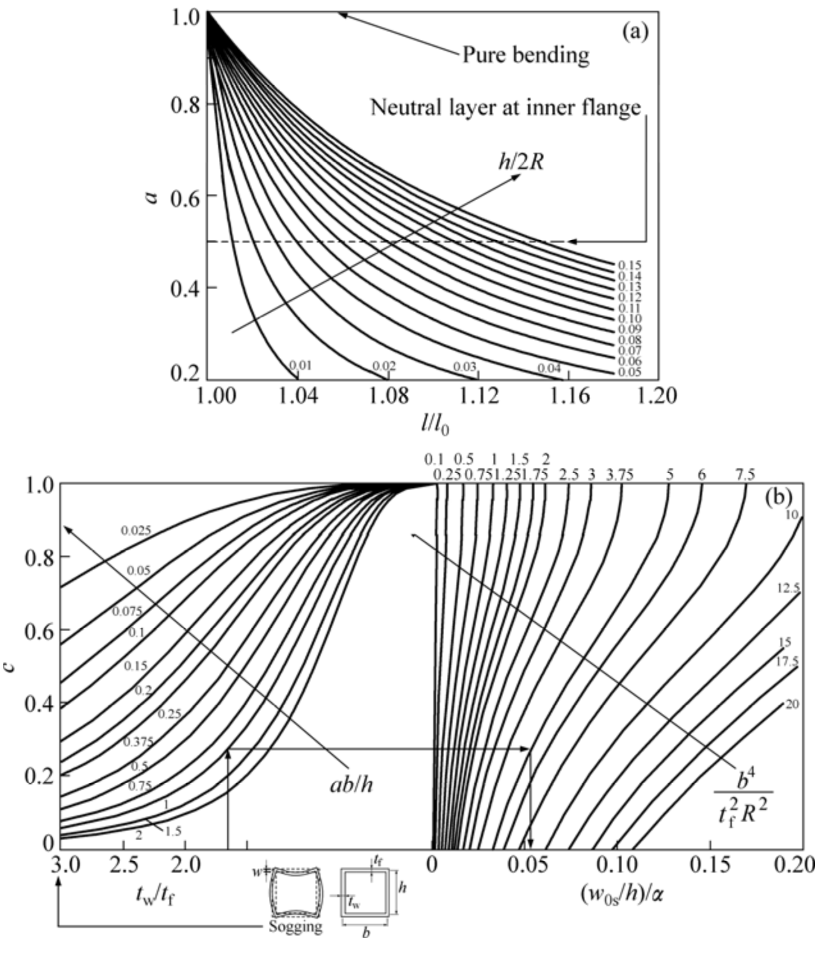

Fig.8 Practical design procedure for evaluation of magnitude of sagging: (a) Influence factor of tension (a) on flange sagging; (b) Maximum sagging depth for SC sections

forming is mass conservation. Due to (primarily) a one dimensional state of stress, the dimensions in the plane of the cross section of a profile exposed to stretch in the longitudinal direction do shrink. In stretch forming, when the entire cross section is exposed to stretching, the characteristic dimensions of the cross section will change considerably due to mass conservation. If the material is isotropic, and the average stretch across the section is, say, 5%, a rectangular hollow section (80 mm × 80 mm × 3 mm) will contract into a trapezoidal section with a depth of 78 mm and a minimum width of 76 mm, if the neutral layer is located inside the inner flange. These dimensional changes are nominal and have to be considered by the product development team as a part of the GD&T process. What is more challenging, however, is if other factors (extrusion die design from different tool makers, material flow, etc) cause variations in the normal anisotropy of the material, they will subsequently cause variations in cross-sectional dimensions.

5.2 Model for prediction of local distortions

5.2.1 Anisotropic material model

Due to the basic characteristic of the problem to be analyzed herein, material's anisotropy is a factor that affects the amount of local deformations in bending. Therefore, this feature was included using Hill's yield criterion[3]:

$$f(\sigma_{ij})=\frac{3}{2}\frac{1}{F+G+H}[(\sigma_y-\sigma_z)^2+G(\sigma_z-\sigma_x)^2+ H(\sigma_x-\sigma_y)^2+2L\sigma_{yz}^2+2M\sigma_{zx}^2+2N\sigma_{xy}^2]=\overline{\sigma}^2 \tag{3}$$

where f is the yield function, $\overline{\sigma}$ is effective stress, σ_{ij} represents individual stress components, and F, G, H, L, M and N are parameters characterizing the current state of anisotropy. The specific application of Eq.(3) will be adapted to the following conditions[4]:

1) Pure plastic deformations (neglecting elastic deformations);

2) Two principal axes of asymmetry only the yield stress in the x-direction ($\overline{\sigma}_x$) is generally different from the yield stress in the two other directions, y and z ($\overline{\sigma}_y=\overline{\sigma}_z\neq\overline{\sigma}_x$);

3) A state of plane stress (σ_z=0);

4) The shear stresses are small and are consequently neglected in the constitutive equation; i.e., the direction of principal stresses coincides with the axes of the (local) Cartesian coordinate system chosen;

5) Defining a single anisotropy parameter, $r\equiv(\mathrm{d}\varepsilon_{xx}^{\mathrm{p}}/\mathrm{d}\varepsilon_{zz}^{\mathrm{p}})$, in which $\mathrm{d}\varepsilon_{xx}^{\mathrm{p}}$ and $\mathrm{d}\varepsilon_{zz}^{\mathrm{p}}$ are the plastic strain increments taken in the section of a uniaxial test specimen with the stress applied in the y-direction.

Then, the yield function takes the following form:

$$f(\sigma_{ij})=\frac{3}{2}\frac{1}{(2r+1)}[2r\sigma_x^2+(1+r)\sigma_y^2-r\sigma_x\sigma_y]=\overline{\sigma}^2 \tag{4}$$

Using the deformation theory of plasticity, it may be shown that the individual stress components can be expressed in terms of the plastic strain components by the following expressions:

$$\sigma_x=\frac{1+2r}{r(2+r)\lambda}[(1+r)\varepsilon_x^{\mathrm{p}}+r\varepsilon_y^{\mathrm{p}}] \tag{5}$$

$$\sigma_y=\frac{1+2r}{(2+r)\lambda}[2\varepsilon_y^{\mathrm{p}}+\varepsilon_x] \tag{6}$$

where λ is a scalar multiplier defined as

$$\lambda=\frac{3\overline{\varepsilon}^{\mathrm{p}}}{2\overline{\sigma}} \tag{7}$$

in which the equivalent plastic strain ($\overline{\varepsilon}^{\mathrm{p}}$) based on these assumptions takes the form

$$(\overline{\varepsilon}^{\mathrm{p}})^2=\frac{2}{3}\frac{1+2r}{r(r+2)^2}[r(2\varepsilon_y^{\mathrm{p}}+\varepsilon_x^{\mathrm{p}})^2+ (r\varepsilon_y^{\mathrm{p}}+(1+r)\varepsilon_x^{\mathrm{p}})^2+(\varepsilon_x^{\mathrm{p}}-r\varepsilon_y^{\mathrm{p}})^2] \tag{8}$$

and, finally, the relationship between equivalent strain and stress can be represented by the simple two-parameter power law[5]:

$$\overline{\sigma}=K(\overline{\varepsilon}^{\mathrm{p}})^n \tag{9}$$

where K is the so-called strength factor and n is the strain hardening coefficient.

5.2.2 Moment-curvature relation for an anisotropic sheet

During bending of a profile, the stress state of the (external) tensile flange resembles the one of a thin-walled sheet subjected to the combination of an axial force (n_x=$\sigma_x t$) in the longitudinal direction (x) and a bending moment (m_x) that provides bending deformations in the perpendicular direction (y) (see Fig.9). The former is due to global bending stresses, whereas the latter is due to the global curvature of the profile (flange). If the thickness (t) of the sheet is much smaller than the depth of the cross section (H), and the bending radius (R_y) is much larger than H, the strain ($\varepsilon_x^{\mathrm{p}}$) may be assumed constant across the thickness of the sheet and equal to the global bending strain $\varepsilon_{x0}^{\mathrm{p}}$ at the median plane of the sheet (see Fig. 9); hence,

$$\varepsilon_{x0}^{\mathrm{p}}=\frac{z_0}{R_y};\quad \varepsilon_{y0}^{\mathrm{p}}=-\frac{1}{2}\frac{z_0}{R_y}=\varepsilon_{z0}^{\mathrm{p}} \tag{10}$$

due to incompressibility along with the assumption made above, $\overline{\sigma}_y=\overline{\sigma}_z$. Here z_0 is the instantaneous distance from the 'neutral layer' of the profile's cross section to the median plane of the sheet. Defining the local curvature (κ_x) about the x-axis perpendicular to the

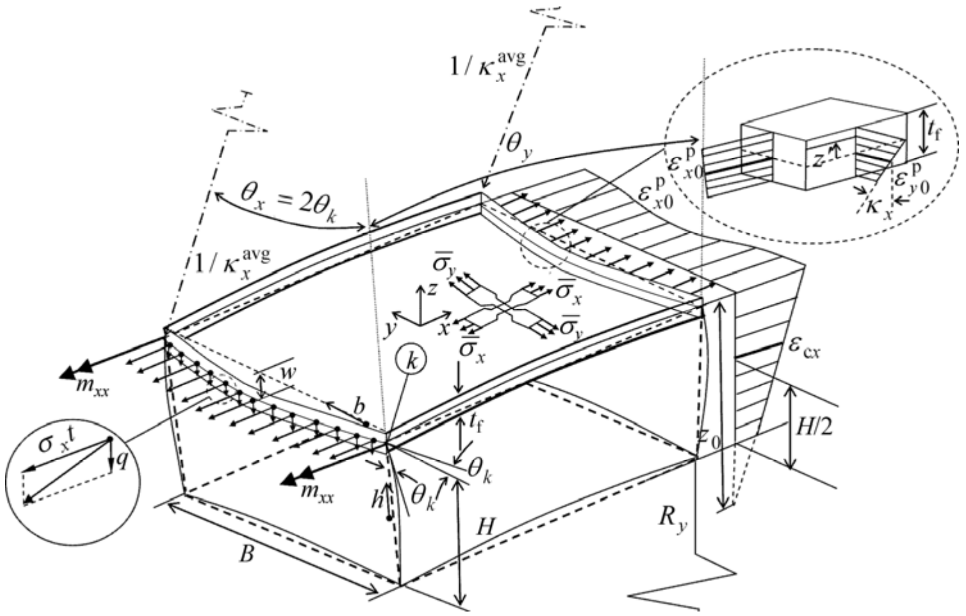

Fig.9 Analytical model for prediction of sagging

global bending axis (y), the following relationship holds

$$\varepsilon_y^{\mathrm{p}} = \kappa_x z' - \varepsilon_{x0}^{\mathrm{p}}/2 \tag{11}$$

where z' is the distance taken from the median plane to an arbitrary layer of the sheet. Combining Eqs.(6), (10) and (11), the local bending stress is then given by

$$\sigma_y = \frac{1+2r}{(2+r)\lambda}\left[2\kappa_x z'\right] \tag{12}$$

Since the flange (sheet) is free to move in the width (y) direction and there are usually no forces applied from the tool in this direction, the local bending moment (per unit length) can be obtained by evaluating the following integral:

$$m_x = \int_{-t/2}^{t/2} \sigma_y z' \mathrm{d}z' = \int_{-t/2}^{t/2} \frac{1+2r}{(2+r)\lambda}\left[2\kappa_x (z')^2\right]\mathrm{d}z' \tag{13}$$

Since the global bending strain ($\varepsilon_{x0}^{\mathrm{p}}$) is usually much larger than the local bending strain ($\approx \kappa_x t/2$), an approximate solution may be obtained by neglecting higher order terms of ($\kappa_x t/2\varepsilon_{x0}^{\mathrm{p}}$). After some simplifications, one obtains the following moment−curvature relationship for an anisotropic flange under the action of global bending:

$$\kappa_x = \frac{3}{4}\frac{m_x(\varepsilon_{x0}^{\mathrm{p}})^{1-n}}{KI}\psi_{\mathrm{m}}(r)$$

$$\psi_{\mathrm{m}}(r) = \frac{2+r}{1+2r}\left[\frac{1}{3}\sqrt{3(2+1/r)}\right]^{1-n} \tag{14}$$

where $I=t^3/12$ is the second moment of inertia (per unit length) of the sheet.

5.2.3 Deformations of curved, thin-walled flange

The local analysis model consists of a curved, thin-walled sheet (flange) subjected to axial stretching and transverse bending due to an internal load q. The system is rather complex due to geometrical and mechanical non-linearities, which influence the instantaneous stiffness and loading conditions. An approximate engineering method will therefore be employed.

Assuming the global bending strain to vary linearly across the depth of the cross section (Bernoulli-Navier), the longitudinal strain component taken at the median plane of the flange is (see Fig. 9)

$$\varepsilon_{x0}^{\mathrm{p}} = \varepsilon_{\mathrm{c}x} + \frac{H-2w}{2R_y} \tag{15}$$

where $\varepsilon_{\mathrm{c}x}$ is the nominal bending strain at the mid-depth of the cross section, H is the depth of the cross section, R_y is the global bending radius and w is the local deflection.

Considering equilibrium of the curved flange, an internally distributed load $q=\sigma_x t/R_y$ introduces transverse bending of the flange. Using the anisotropic material model discussed above, the internally distributed load is

$$q = K\left(\frac{1+2r}{3r}\right)^{\frac{n}{2}-1}\varepsilon_x^n \frac{t}{R_y} =$$

$$K\left(\frac{1+2r}{3r}\right)^{\frac{n}{2}-1}\left(\varepsilon_{\mathrm{c}x} + \frac{H-2w}{2R_y}\right)^n \frac{t}{R_y} \tag{16}$$

Assuming small local deflections ($\mathrm{d}w/\mathrm{d}y$<<1), the local bending curvature may be approximated with the second derivative of the displacement, hence,

$$\frac{\partial^2 w}{\partial y^2}=\frac{3}{4}\frac{m_x(\varepsilon_{x0}^{\mathrm{p}})^{1-n}}{KI}\psi_{\mathrm{m}}(r) \tag{17}$$

Differentiating this equation twice with respect to y gives

$$\frac{KI}{\psi_{\mathrm{m}}(r)}\frac{4}{3}\frac{\partial^4 w}{\partial y^4}=-q\varepsilon_{x0}^{1-n}+2Q\frac{\partial(\varepsilon_{x0}^{1-n})}{\partial y}+m_x\frac{\partial^2(\varepsilon_{x0}^{1-n})}{\partial y^2} \tag{18}$$

where Q is the internal shear force obtained from equilibrium and m_x is the (local) bending moment. It may be noticed that all three terms on the right hand side of Eq.(18) are functions of the displacement (w). However, since $w<<H$, the relative influence of w on each individual term is minor. This may justify replacing w with a polynomial in those three terms. Successively, integrating Eq.(18) and applying boundary conditions for a rectangular hollow section, the result may, after some simplifications, be approximated with a closed-form expression in the form:

$$w=\psi_{\mathrm{m}}\psi_{\mathrm{c}}\psi_{\mathrm{s}}\frac{HB^4}{t_{\mathrm{f}}^2 R_y^2} \tag{19}$$

where t_{f} is flange thickness, ψ_{m} defines the effect of anisotropy, see Eq.(14), and ψ_{c} and ψ_{s} express the effects of constraints between individual members and external stretching, respectively. The applicability of Eq.(19) is more general than that of the model suggested by ZHU et al[6].

5.2.4 Validation of sagging model for anisotropic material

In the full scale rotary stretch forming tests done, the extreme ends of an extruded profile were clamped to the die, using two bolts at each end, and imposing simultaneous stretching and bending by means of an external press, counter rotating two semi-dies about individual pivot points (see Fig.4(a)). Die sets with two different geometries (centre die radius of 1 600 mm and 450 mm, respectively) were used in the work. A simple computer routine was used to calculate the pivot point position, profile's cut length and bending angle in order to provide the desired stretch level, as represented by the engineering strain at the mid-depth of the section ($4.4\% \le \varepsilon_{\mathrm{c}x} \le 6.4\%$). Once the bend angle was completed, unloading was performed and the clamp was released. The bent profile was then put in a fixture for measurements of characteristic dimensions, including sagging depth (w) (see Fig.10).

Rectangular hollow extrusions (60 mm × 40 mm × 4.0 mm) in alloy AA7108-W were used in the experiments, following industrial heat treatment practices. Material data were: 630 MPa $\le K \le$ 757 MPa; $1.20 \le r \le 2.11$; $0.33 \le n \le 0.35$.

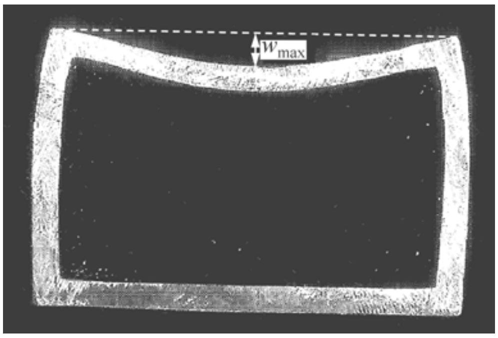

Fig.10 Photograph of deformed section in profile's centre

The impact of geometrical parameters on sagging of the external flange is illustrated for different degrees of anisotropy in Fig.11. The analytical model (full lines) predicts an almost linear relationship between sagging and the defined parameter, $B^4/(R_y^2 t_{\mathrm{f}}^2)$, when w/H<0.1 for different r-values. This means that the considered parameter is the main design parameter with regard to the amount of nominal deflection of the flange in rotary stretch bending. The width of the flange (B) is the most important design parameter, whereas the flange thickness (t_{f}) is the main source to noise since this shows the highest relative variability in the upstream process steps. The anisotropy factor, $r=\mathrm{d}\varepsilon_{xx}^{\mathrm{p}}/\mathrm{d}\varepsilon_{zz}^{\mathrm{p}}$, is the major material characteristic with regard to sagging depth (K and n do have minor impact on sagging). The results show that sagging decreases with increasing r. In other words, if the yield strength in the width direction ($\bar{\sigma}_y$) increases relative to the yield stress in the length direction ($\bar{\sigma}_x$), the local distortion (sagging) of the external flange decreases.

Fig.12 shows the effects of anisotropy and stretching on local distortions ($\varepsilon_{\mathrm{c}x}$ is the longitudinal strain taken at the mid-depth of the cross section). Notice that $\varepsilon_{\mathrm{c}x}$=6.4% corresponds to an average strain of 2.0% at

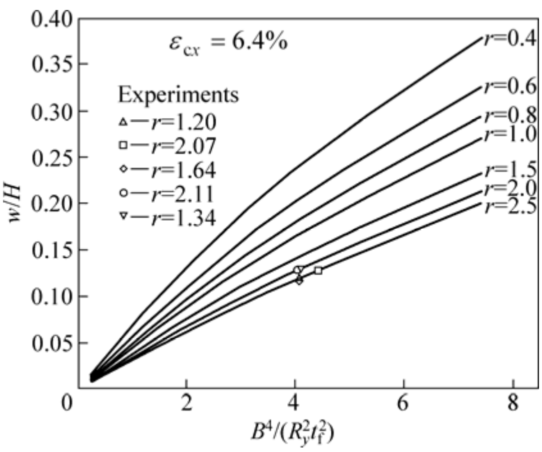

Fig.11 Normalized sagging depth (w) for different anisotropy parameters (r)

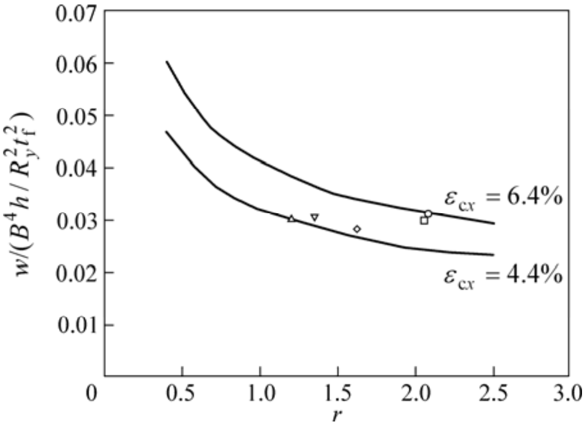

Fig.12 Sagging depth for different anisotropy parameters (r) and stretch levels (ε_{cx})

the inner fiber. These results show that increased stretch level does increase sagging, meaning that appropriate stretch is an important design parameter for stretch forming tools. Moreover, dimensional product variability may be expected if the upstream processing steps introduce different states of anisotropy prior to forming. The agreement between experimental and analytical results is surprisingly good.

6 Conclusions

1) The different manufacturing companies' capability of developing and industrializing new forming technology is a characteristic property with regard to their competitiveness in the future.

2) Improved understanding of forming mechanisms combined with models that relate process parameters to product quality are key enablers for innovation in the metal forming industry.

3) Rotary stretch forming is a typical example on new technology that has proven to dramatically improve dimensional accuracy of formed products.

4) An approach to control local bend accuracy, which is primarily influenced by sagging of cross-sectional members, includes controlling mechanisms and parameters in those specific process steps (e.g. extrusion process) that influence thickness and anisotropy of cross-sectional members.

References

[1] WELO T. Bending of aluminum extrusions for automotive applications: A commentary on theoretical and practical aspects [C]// Proc 6th Int Aluminium Extrusion Technology Seminar. Chicago, USA, 1996: 271.

[2] PAULSEN F, WELO T. Cross-sectional deformations of rectangular hollow sections in bending: Part II—Analytical models [J]. Int Journal of Mechanical Sciences, 2001, 43: 131−152.

[3] HILL R. The mathematical theory of plasticity [M]. Oxford: Oxford Engineering Science Series, 1950.

[4] WELO T, BARINGBING H A. On the evaluation of dimensional accuracy in rotary stretch bending [C]//12th Int Esaform Conference on Material Forming. Twente, The Netherlands, 2009.

[5] LUDWIK P. Technologische studie über blechbiegung [J]. Technische Blatter, 1903: 133−159.

[6] ZHU H, STELSON K A. Distortion of rectangular tubes in stretch bending [J]. Transactions of the ASME, 2002, 124: 886−890.

(Edited by YANG Bing)